RSC Advances

This article can be cited before page numbers have been issued, to do this please use: Z. H. Zhang, W. Jiang, X. X. Ban, M. Yang, S. Ye, B. Huang and Y. Sun, *RSC Adv.*, 2015, DOI: 10.1039/C5RA00627A.

ROYAL SOCIETY OF CHEMISTRY

www.rsc.org/advances

View Article Online
DOI: 10.1039/C5RA00627A

Solution-processed Efficient Deep-Blue Fluorescent Organic Light-Emitting Diodes Based On Novel 9,10-diphenyl-anthracene Derivatives

Zhaohang Zhang,[a] Wei Jiang,[*a] Xinxin Ban,[a] Min Yang,[b] Shanghui Ye,[*b] Bin Huang,[a] and Yueming Sun,[*a]

[a] School of Chemistry and Chemical Engineering, Southeast University, Nanjing, 210096, Jiangsu, P. R. China

[b] Institute of Advanced Materials (IAM) Nanjing University of Posts & Telecommunications (NUPT), 9 Wenyuan Road, Nanjing, 210023, Jiangsu, P. R. China

Corresponding authors:

[*]e-mail: 101011462@seu.edu.cn (W. Jiang); e-mail: iamshye@njupt.edu.cn (S. Ye); e-mail: sun@seu.edu.cn (Y. Sun).

View Article Online
DOI: 10.1039/C5RA00627A

Abstract

A series of 9,10-diphenyl-anthracene derivatives bearing either benzimidazole or carbazole moieties as substituents materials were synthesized and characterized as blue emitters for organic light-emitting diodes (OLEDs). Their optical, electrochemical and thermal properties have been investigated, and their molecular structure-property relationships were evaluated. These compounds both exhibited high glass-transition temperature ($T_g \geq$ 195 °C) and high decomposition temperature ($T_d \geq$ 494 °C). The solution processed non-doped device using CAC for fluorescence emitter showed a maximum luminance efficiency of 1.63 cd/A, a maximum power efficiency of 0.77 lm/W and a maximum external quantum efficiency of 1.53 %. By introducing 1,3-bis[4-*tert*-butylphenyl-1,3,4-oxadiazolyl] phenylene (OXD-7) :Polyvinylcarbazole (PVK) as host in the emitting layer, the doped deep-blue emitting device of CAC exhibited a turn-on voltage of 4.75 V, a maximum luminance efficiency of 3.03 cd/A, a maximum power efficiency of 1.64 lm/W and a maximum external quantum efficiency of 2.81 %. Our results demonstrate a promising approach to well-designed materials for use in deep-blue fluorescence OLED applications.

Key words Anthracene, Carbazole, Benzimidazole, Solution processed, Blue fluorescence

View Article Online
DOI: 10.1039/C5RA00627A

Introduction

Organic light emitting diodes (OLEDs) have been extensively studied for applications in full-color flat-panel displays and lighting sources owing to their ability to be driven by low voltages, have high brightness, and be easily fabricated in large area and thin film devices.[1-5] The development of deep-blue, is of special significance because such emitters could be utilized to generate light of other colors by energy cascading to a lower-energy fluorescent.[6] Recently, numerous materials have been developed to be used as blue emitter, and some of them exhibited excellent performance.[7-9] The performance of blue electroluminescence (EL) devices needs to be further improved in terms of efficiency, lifetime and color purity owing to the far superior stabilities and device performances of green and red emitters. The synthesis of blue fluorescence materials with multiple functions, such as high emissive efficiency, transport properties and balanced charge injection, good morphological and thermal stability, still remains one of the most challenging areas in this field.

Anthracene has been intensively studied as an attractive starting material, due to its unique chemical and electron-rich structure, low electronic band gap and strong blue fluorescence, and also used as blue emitters in OLEDs.[10-12] The anthracene can be easily modified though directly introducing different functionalized blocks at the 9,10-positions because of the electron-rich properties and large p-conjugation system which enhance the separated energy levels of HOMO and LUMO, as well as can be used in solution-processed devices. The phenyl rings and anthracene core were applied as linker, which will reduce the substituent group interactions between 9,10-positions and solve the problems of huge bathochromic effect and low quantum yield.[13] Therefore, the devices containing diphenylanthracene as an emitter are

View Article Online
DOI: 10.1039/C5RA00627A

expected to show higher electroluminescence efficiency, long lifetime, and deep blue color. Furthermore, carbazole-based molecules have been widely used as blue fluorescence OLEDs due to their high triplet energy and excellent hole-transporting properties.[14-17] The introduction of the hole-transporting carbazole moiety into a molecule can significantly enhance the glassy-state durability, thermal stability and the electro-optical properties of organic compounds.[18-21] On the other hand, the electron-transporting materials are structurally more diverse such as tris(8-hydroxyquinolinato) aluminum(III) (Alq_3),[1] oxadiazole, triazole derivatives and other nitrogen-containing electro-deficient materials.[22,23] Benzimidazole group was introduced to the material as an electron acceptor due to its high electron affinity.[24,25]

In this paper, we synthesized a series of blue lighting materials containing carbazole moiety and benzimidazole moiety of the 9,10-diphenyl-anthracene derivatives, 9,10-bis(3',5'-bis(1-phenyl-1H-benzo[d]imidazol-2-yl)biphenyl-4-yl)-anthracene (CAC), 9,10-bis(3,6-Bis(3,6-di-tert-butyl-carbazol-9-yl)-carbazole)biphenyl-4-yl)-anthracene (BAB) and 9-[4-(3,6-Bis(3,6-di-tert-butylcarbazol-9-yl)-carbazole)-phenyl]-10-[4-(3',5'-bis(1-phenyl-1H-benzo[d]imidazol-2-yl))-phenyl]-anthracene (BAC). As shown in the **Scheme 1**, it is particularly intriguing to compare the electroluminescent properties of CAC, BAB and BAC, all possessing the same molecular structure containing 9,10-diphenyl-anthracene units. We only changed the connecting substituent group of carbazole and/or benzimidazole. The color and energy levels were modified by the phenyl bridge between the functionalized moieties and the anthracene core. The thermal properties and photophyscial properties were fully

View Article Online
DOI: 10.1039/C5RA00627A

investigated. The HOMO and LUMO values were measured by cyclic voltammetry. In addition, a series of devices were fabricated to systematically study the emitting properties of these 9,10-diphenyl-anthracene derivatives. We achieved a current efficiency of 3.03 cd/A, a maximum power efficiency of 1.64 lm/W, a maximum external quantum efficiency of 2.81 % and a maximum brightness of 3490 cd/m^2 with a deep-blue CIE (0.16, 0.10) in a doped device for CAC.

Experimental

General

All reactants and solvents, unless otherwise stated, were purchased from commercial sources and used as received. ^{1}H NMR and ^{13}C NMR spectra were recorded on a Bruker ARX300 NMR spectrometer with tetramethylsilane as the internal standard. Mass spectrometry was performed with a Thermo Electron Corporation Finnigan LTQ mass spectrometer. Elemental analysis was performed on an Elementar Vario EL CHN elemental analyzer. Absorption spectra were recorded with a UV-vis spectrophotometer (SHIMADZU 2450) and PL spectra were recorded with a fluorospectrophotometer (HORIBA, FL3-2iHR). Thermogravimetric analysis (TGA) was performed using a Netzsch simultaneous thermal analyzer (STA) system (STA 409PC) under dry nitrogen atmosphere at a heating rate of 10 °C/min. Glass-transition temperature was recorded by DSC at a heating rate of 10 °C/min with a thermal analysis instrument (DSC 2910 modulated calorimeter). Cyclic voltammetry were performed on a Princeton Applied Research potentiostat/galvanostat model 283 voltammetric analyzer in CH_2Cl_2 solutions (10^{-3} M) (oxidation process) or acetonitrile

View Article Online
DOI: 10.1039/C5RA00627A

solution (10^{-3} M) (reduction process) at a scan rate of 100 mV/s with a platinum plate as the working electrode, a silver wire as the pseudo-reference electrode, and a platinum wire as the counter electrode. The supporting electrolyte was tetrabutylammonium hexafluorophosphate (0.1 M) and ferrocene was selected as the internal standard. The solutions were bubbled with a constant argon flow for 10 min before measurements.

Device fabrication and performance measurements

Blue OLED devices using CAC, BAB and BAC as EML with structure ITO/PEDOT:PSS(30 nm)/EML(20 nm)/TPBI(35 nm)/Ca(10 nm):Ag(100 nm) and ITO/PEDOT:PSS(30 nm)/PVK:OXD-7(7:3):EML(5 wt%, 10 wt%, 15 wt%, 20 wt%)(20 nm)/TPBI(35 nm)/Ca(10 nm):Ag(100 nm) using Polyvinylcarbazole (PVK): 1,3-bis[4-*tert*-butylphenyl-1,3,4-oxadiazolyl]phenylene (OXD-7) as mixed host were fabricated and characterized as follows. In a general procedure, indium-tin oxide (ITO)-coated glass substrates were pre-cleaned carefully and treated by UV ozone for 4 min. A 30 nm poly(3,4-ethylenedioxythiophene) doped with poly(styrene-4-sulfonate)(PEDOT:PSS) aqueous solution was spin coated onto the ITO substrate and baked at 210 °C for 10 min. The substrates were then taken into a nitrogen glove box, where emitting layer was spin coated onto the PEDOT:PSS layer from chlorobenzene solution and annealed at 120 °C for 30 min. The substrate was then transferred into an evaporation chamber, where the TPBI was evaporated at an evaporation rate of 1–2 Å/s under a pressure of 8×10^{-5} Pa and the Ca/Ag bilayer cathode was evaporated at evaporation rates of 1 and 3 Å/s for Ca and Ag,

View Article Online
DOI: 10.1039/C5RA00627A

respectively, under a pressure of 4×10^{-4} Pa. The current-voltage characteristics of the devices were characterized with Keithley 2602 semiconductor characterization system and the brightness characteristics of the devices was characterized with Si-photodiode characterization system. The electroluminescent spectra were collected with a Photo Research PR655 Spectrophotometer. All measurements of the devices were carried out in ambient atmosphere without further encapsulations.

Quantum chemical calculations

The geometrical and electronic properties of CAC, BAB and BAC were performed with the Gaussian 03 program package.[26] The calculation was optimized at the B3LYP/6-31G(d) level of theory. The molecular orbitals were visualized using Gaussview.

Materials

Compounds Synthesis: The benzimidazole **1** and **2** was prepared according to published procedures.[27] The carbazole dendrons **3** were synthesized according to the literature methods.[28,29] The compounds **4** was synthesized by already known reduction procedure developed by Smet et al.[30]

Synthesis of 2,2'-(5-bromo-1,3-phenylene)bis(1-phenyl-1H-benzo[d]imidazole) (1). The mixture of 5-Bromo-benzene-1,3-dicarbaldehyde (2.13 g, 10 mmol), 2-Aminodiphenylamine (4.6 g, 25 mmol) was dissolved in DMF (20 mL). A solution of disodiummetabisulfite (3.8 g 20 mmol) in water (10 mL) was added slowly. The mixture was stirred at 80 °C for 12 h. After cooling to room temperature, the solvent was removed by suction filtration and the residue was extracted with dichloromethane.

View Article Online
DOI: 10.1039/C5RA00627A

The product was then obtained by column chromatography on silica gel with petroleum ether/ dichloromethane/ethyl acetate (5:5:1) as the eluent, to yield a white solid (3.5 g, 65 %). ^{1}H-NMR (500 MHz, $CDCl_3$, δ): 7.87-7.85 (m, 4H), 7.53 (s, 1H), 7.51–7.44 (m, 6H), 7.34 (t, J = 7.6 Hz, 2H), 7.28 (d, J = 7.5 Hz, 2H), 7.19 (t, J = 6.9 Hz, 6H). ^{13}C-NMR (300 MHz, $CDCl_3$, δ): 149.74, 149.45, 137.12, 136.10, 133.35, 130.08, 129.09, 128.47, 127.34, 123.97, 123.43, 122.53, 119.99, 110.62. MS (MALDI-TOF) [m/z]: calcd for $C_{32}H_{21}N_4Br$, 540.1; found, 540.6. Anal. Calcd. for $C_{32}H_{21}N_4Br$: C, 70.99; H, 3.91; N 10.35. Found: C, 70.85; H, 3.94; N 10.26.

Synthesis of 2,2'-(5-(4,4,5,5-tetramethyl-1,3,2-dioxaborolan-2-yl)-1,3-phenylene) bis(1-phenyl-1H-benzo[d]imidazole) (2). The mixture of **1** (1.03 g, 1.9 mmol), bis(pinacolato)diboron (0.53 g, 2.1 mmol), $Pd(dppf)Cl_2$ (0.06 g, 0.05 mmol), anhydrous potassium acetate (0.4 g, 4 mmol), and dried DMF 20 mL was refluxed under an nitrogen atmosphere for 24 h at 80 °C. After the reaction finished, the reaction mixture was extracted with dichloromethane and washed with water. The organic layer was dried by anhydrous $MgSO_4$ and filtered. The product was isolated by silica gel column chromatography using petroleum ether/ dichloromethane/ethyl acetate (5:5:1) as eluent to afford a white solid (1.02 g, 76 %). ^{1}H NMR (300 MHz, $CDCl_3$, δ): 8.20 (s, 2H), 7.88 (d, J = 7.9 Hz, 2H), 7.50 (s, 1H), 7.43-7.21 (m, 12H), 7.16 (d, J = 7.2 Hz, 4H), 1.27 (s, 12H). ^{13}C-NMR (300 MHz, $CDCl_3$, δ): 137.23, 129.84, 128.78, 127.46, 123.56, 119.76, 110.52, 84.09, 24.80. MS (MALDI-TOF) [m/z]: calcd for $C_{38}H_{33}BN_4O_2$, 588.3; found, 588.6. Anal. Calcd. for $C_{38}H_{33}BN_4O_2$: C, 77.55; H, 5.65; N 9.52. Found: C, 77.45; H, 5.70; N 9.56.

View Article Online
DOI: 10.1039/C5RA00627A

Synthesis of 9,10-bis(3',5'-bis(1-phenyl-1H-benzo[d]imidazol-2-yl)biphenyl-4-yl)-anthracene (CAC). The mixture of 9,10-Bis-(4-bromo-phenyl)-9,10-dihydro-anthracene (0.488 g, 1 mmol), **3** (1.8 g, 2.5 mmol), cuprous iodide (0.5 g, 2.63 mmol), 1,10-Phenanthroline hydrate (0.5 g, 2.52 mmol), potassium carbonate (0.83 g, 6 mmol), and dried DMF 20 mL was refluxed under an nitrogen atmosphere for 24 h at 160 °C. After the reaction finished, the reaction mixture was extracted with dichloromethane and washed with water. The product was isolated by silica gel column chromatography using petroleum ether/ ethyl acetate (50:1) as eluent to afford a yellow solid (1.05 g, 60 %). ^{1}H NMR (300 MHz, $CDCl_3$, δ): 8.32 (s, 4H), 8.19 (s, 8H), 8.06 (d, J=8.1 Hz, 4H), 7.98-7.88 (m, 12H), 7.73 (dd, J = 8.7, 1.8 Hz, 4H), 7.55 (q, J = 3.3 Hz, 4H), 7.51 (d, J = 1.5 Hz, 4H), 7.48 (d, J = 1.5 Hz, 4H), 7.4 (d, J = 8.4 Hz, 8H), 1.48 (s, 72H). ^{13}C-NMR (300 MHz, $CDCl_3$, δ): 142.13, 139.91, 139.66, 138.37 , 135.90, 132.70, 130.62, 129.58, 126.61, 126.40, 125.60, 125.19, 123.71, 123.09, 122.68, 118.94, 115.76, 110.83, 108.64, 34.26, 31.57. MS (MALDI-TOF) [m/z]: calcd for $C_{130}H_{124}N_6$, 1769.0; found, 1768.6. Anal. Calcd. for $C_{130}H_{124}N_6$: C, 88.19; H, 7.06; N 4.75. Found: C, 88.05; H, 6.98; N 4.81.

Synthesis of 9,10-bis(3,6-Bis(3,6-di-tert-butylcarbazol-9-yl)-carbazole)biphenyl-4-yl)-anthracene (BAB). The mixture of 9,10-Bis-(4-bromo-phenyl)-9,10-dihydro-anthracene (0.244 g, 0.5 mmol), **2** (0.7 g, 1.2 mmol), potassium carbonate (0.7 g, 5 mmol), terakis(triphenylphosphine)palladium (0.1 g, 0.08 mmol) was dissolved in 20 mL mixture solution of toluene: ethanol: water (6:3:1) and refluxed under nitrogen for 24 h at 80 °C. After the reaction finished, the reaction mixture was extracted with

View Article Online
DOI: 10.1039/C5RA00627A

dichloromethane and washed with water. The product was isolated by silica gel column chromatography using petroleum ether/ dichloromethane/ethyl acetate (5:5:1) as eluent to afford a yellow solid (0.45 g, 72 %). ^{1}H NMR (300 MHz, $CDCl_3$, δ): 8.04 (s, 2H), 7.92 (d, J = 8.7 Hz, 8H), 7.68 (dd, J = 6.9, 3 Hz, 4H), 7.59-7.49 (m, 12H), 7.45 (d, J = 8.1 Hz, 4H), 7.35 (d, J = 7.5 Hz, 18H), 7.31 (d, J = 5.1 Hz, 10H). ^{13}C-NMR (300 MHz, $CDCl_3$, δ): 150.93, 140.32, 138.18, 138.15, 136.64, 136.31, 136.08, 131.23, 130.29, 129.58, 129.32, 128.82, 128.29, 127.12, 126.52, 126.37, 124.66, 123.16, 122.72, 119.54, 110.06. MS (MALDI-TOF) [m/z]: calcd for $C_{90}H_{58}N_8$, 1250.48; found, 1250.82. Anal. Calcd. for $C_{90}H_{58}N_8$: C, 86.37; H, 4.67; N 8.95. Found: C, 86.22; H, 4.53; N 8.97.

Synthesis of 9-[4-(3,6-Bis(3,6-di-tert-butylcarbazol-9-yl)-carbazole)-phenyl]-10-[4-(3',5'-bis(1-phenyl-1H-benzo[d]imidazol-2-yl))-phenyl]-anthracene (BAC). The **5** was synthesized by the same procedure like **CAC** through change the mixture ratio of 9,10-Bis-(4-bromo-phenyl)-9,10-dihydro-anthracene (1.22 g, 2.5 mmol) and **3** (0.72 g, 1 mmol). The 1.0 g mixture products of **5** and **CAC**, **2** (0.7 g, 1.2 mmol), potassium carbonate (0.7 g, 5 mmol), terakis(triphenylphosphine)palladium (0.1 g, 0.08 mmol) were dissolved in 15 mL mixture solution of toluene: ethanol: water (6:3:1) and refluxed under nitrogen for 24 h at 80 °C. After the reaction finished, the reaction mixture was extracted with dichloromethane and washed with water. The product was isolated by silica gel column chromatography using petroleum ether/dichloromethane/ethyl acetate (5:5:1) as eluent to afford a yellow solid (0.7 g, 50 %). ^{1}H NMR (300 MHz, $CDCl_3$, δ): 8.31 (s, 2H), 8.18 (s, 4H), 8.03-7.83 (m, 14H),

View Article Online
DOI: 10.1039/C5RA00627A

7.73 (t, J = 9.0 Hz, 4H), 7.57-7.48 (m, 15H), 7.41-7.30 (m, 16H), 1.48 (s, 36H). ^{13}C-NMR (300 MHz, $CDCl_3$, δ): 150.76, 142.11, 139.92, 139.68, 138.17, 136.55, 136.20, 132.71, 132.35, 131.25, 130.59, 129.62, 129.44, 128.99, 128.87, 128.83, 128.38, 127.13, 126.62, 126.56, 126.41, 126.21, 125.58, 125.04, 124.82, 124.68, 123.69, 123.29, 123.10, 122.89, 122.85, 122.67, 119.46, 118.92, 118.56, 115.75, 110.84, 110.11, 108.63, 34.26, 31.57. MS (MALDI-TOF) [m/z]: calcd for $C_{110}H_{91}N_7$, 1509.7; found, 1509.2. Anal. Calcd. for $C_{110}H_{91}N_7$: C, 87.44; H, 6.07; N 6.49. Found: C, 87.57; H, 6.02; N 6.38.

Results and Discussion

Synthesis and characterization

The synthesis routes and chemical structures of CAC, BAB, and BAC are shown in **Scheme 1**. Firstly, the reaction of 1-fluoro-2-nitrobenzene and aniline in the presence of potassium fluoride gave N-Phenyl-o-phenylenediamine in 61 % yield, followed by reduction of the nitro group with stannous chloride dihydrate (80 %). The resulting diamine derivative reacted with 5-Bromo-benzene-1,3-dicarbaldehyde to produce the 2,2'-(5-bromo-1,3-phenylene)bis(1-phenyl-1H-benzo[d]imidazole) (**1**) in 65% yield. **1** was converted to the aryboronic ester of 2,2'-(5-(4,4,5,5-tetramethyl-1,3,2-dioxaborolan-2-yl)-1,3-phenylene)bis(1-phenyl-1H-benzo[d]imidazole) (**2**) catalyzed by $Pd(dppf)Cl_2$ in the presence of CH_3COOK in DMF with a yield of 76 %. Secondly, the key intermediate 3,6-bis(3,6-di-*tert*-butyl-carbazol-9-yl)-car-bazole (**3**) was prepared via a five-step reaction with a total yield of 40%. Thirdly, the compounds **4** was synthesized by

View Article Online
DOI: 10.1039/C5RA00627A

already known reduction procedure.[30] Finally, the target molecules were synthesized via a classic Ullmann reaction and Suzuki reaction respectively. All of the compounds were purified by silica chromatography and recrystallization, producing very pure powders. ^{1}H-NMR, ^{13}C-NMR, mass spectrometry, and elemental analysis were employed to confirm the chemical structures of the above-mentioned compounds, as described in the experimental section.

Thermal analysis

The thermal stabilities of the CAC, BAB and BAC were investigated by thermal gravimetric analyses (TGA) and differential scanning calorimetry (DSC) under nitrogen atmosphere at a heating rate of 10 °C/min. As shown in **Fig. 1**, TGA indicates that CAC, BAB and BAC exhibit decomposition temperature (T_d, corresponding to 5% weight loss) as high as 508, 534 and 494 °C, respectively. The clear glass transition temperature (T_g) values for BAB and BAC are 195 °C and 246 °C, respectively. No noticeable signals related to the crystallization or melting is observed in the DSC curves. The T_g of CAC is not found in the DSC curves, which suggests that CAC could form morphologically stable and uniform amorphous films. As a result, the solution-deposited CAC ET layer has an excellent film-forming property which can be assigned to the favorable solubility of tert-butyl. The excellent thermal properties of these compounds will retain stable film morphological properties during the device operation, which are also desirable for good performance of OLEDs with high efficiency stability.

Electrochemical analysis

View Article Online
DOI: 10.1039/C5RA00627A

The electrochemical properties of CAC, BAB and BAC were studied in solution using cyclic voltammetry (CV) using tetrabutylammonium hexafluorophosphate (TBAPF6) as the supporting electrolyte and ferrocene as the internal standard. As shown in **Fig. 2**, during the anodic scan in dichloromethane, CAC and BAC exhibits similar reversible oxidation process, which can be assigned to the oxidation of electron-donating carbazole moiety, with the onset potentials of 1.21 and 1.24 V, respectively. No reduction waves were detected. The HOMO energy levels were obtained according to the fellow equation: HOMO = -(4.8 + E^{o}_{ox})eV, using ferrocene as an internal standard (-4.8 eV below vacuum). On the basis of the onset potentials for oxidation, we estimated the HOMO energy of CAC and BAC to be -5.23 and -5.26 eV. These results reveal that the introduction of carbazole groups to the anthracene core can lead to the raising of HOMO levels, which are in agreement with the DFT calculations results. BAB and BAC exhibited reduction waves, arising from their benzimidazole moiety, with onset potentials of -2.49, -1.92 V, respectively. These together with absorption spectra were then used to obtain the LUMO energy levels.

Theoretical calculation

The three-dimensional geometries and the frontier molecular orbital energy levels of these anthracene derivatives were calculated using density functional theory (DFT). The calculations of the HOMO and LUMO levels were depicted in **Table 1**. The geometries of these compounds in **Fig. 3** show that the carbazole, benzimidazole and phenyl units are significantly twisted with the anthracene core, resulting in a non-planar structure in each molecule. These geometrical characteristics can

View Article Online
DOI: 10.1039/C5RA00627A

effectively prevent intermolecular interactions between π-systems and thus suppress molecular recrystallization and limit the effective conjugation length of these molecules. As depicted in Fig. 3, The LUMO levels of all the compounds are localized predominantly on the anthracene core, while the HOMO levels of CAC and BAC are distributed over the electron-rich tri-carbazole fragment and BAB is localized on the anthracene core, respectively. Compared with BAB, the HOMO levels of CAC and BAC have increased as the increasing of the generation of the carbazole with the calculated values of -5.04 eV and -5.00 eV, which are more matching with the level of PEDOT:PSS so that reduce the injection of hole and strengthen the device efficiency.

Photophysical properties

Fig. 4 depicts the UV-vis absorption (a) and photoluminescent (b) spectra of CAC, BAB and BAC in CH_2Cl_2 and solid film. **Table 1** summarized the maximal absorption and PL emission wavelengths of the carbazole or/and benzimidazole substituted anthracene derivatives. The absorption spectra of CAC and BAC exhibits two absorption peaks at 242 nm and 298 nm which can be assigned to the π-π* and n-π* transitions of the carbazole moiety respectively, while the absorption peak at 290-300 nm of BAB is attributed to the benzimidazole moieties and the peak at 263 nm can be due to the benzene ring characteristic absorption of BAB. The peaks at 242 nm and 263 nm of BAC indicated the small organic molecule with carbazole and benzimidazole units was synthesized successfully. The common moderately weak absorptions in the range from 350-400 nm can be assigned to the characteristic

View Article Online
DOI: 10.1039/C5RA00627A

vibronic patterns π-π* transition of anthracene.[31] Upon UV excitation, the PL spectrum of CAC, BAB and BAC have lost vibronic structure and the emission peaks red-shifted to 435, 430, and 434 nm, respectively. The band gap was calculated from the edge of the Uv-vis absorption peak, giving values of 3.00, 2.98, and 2.99 eV for CAC, BAB and BAC, respectively. The film fluorescence quantum yields (Φ_F) of CAC, BAB and BAC are 0.87, 0.59 and 0.70, respectively. The results indicates that direct attachment of the carbazole substituent group to the 9,10-diphenyl-anthracene moiety enhanced the Φ_F of CAC and BAC.

Electroluminescence properties

To investigate the EL performance of CAC, BAC and BAB, non-doped fluorescent OLEDs device A and doped fluorescent OLEDs device B were fabricated with a configuration of ITO/PEDOT:PSS(30 nm)/EML(20 nm)/TPBI(35 nm)/Ca(10 nm):Ag(100 nm) and ITO/PEDOT:PSS(30 nm)/PVK:OXD-7(7:3):EML(5 wt%, 10 wt%, 15 wt%, 20 wt%)(20 nm)/TPBI(35 nm)/Ca(10 nm):Ag(100 nm), respectively. The materials structures and the energy level diagrams of the devices are show in **Fig. 5**. In these devices, indium tin oxide (ITO) was used as the anode, poly(3,4-ethylenedioxythiophene) : poly(styrene-4-sulfonate) (PEDOT:PSS) as the hole injection layer, the electron-transporting material 1,3-bis[4-*tert*-butylphenyl-1,3,4-oxadiazolyl]phenylene (OXD-7) mixed into the hole-transporting material Polyvinylcarbazole (PVK) as host in the emitting layer, 1,3,5-tri(phenyl-2-benzimidazolyl)benzene (TPBi) as electron-transporting and hole-blocking layer, and Ca:Ag as the electron injecting layer. All of the important

View Article Online
DOI: 10.1039/C5RA00627A

performance parameters of these OLEDs are summarized in **Table 2**. The electroluminescent (EL) spectra and current density-voltage-luminance (*J-V-L*) characteristics of the devices are shown in **Fig. 6** and **Fig.7**.

Fig. 6 (a) presents the current density-voltage-luminance (*J-V-L*) curves of CAC, BAB and BAC based device A, which turned on at 4.91, 5.80 and 5.49 V (corresponding to 1cd/m^2) and have a maximum brightness (L_{max}) of 3983, 400 and 2945 cd/m^2, respectively. As revealed in Fig. 6 (b), the device A based on CAC shows better performance with the maximum luminance efficiency ($\eta_{c,\,max}$) of 1.63 cd/A, the maximum power efficiency ($\eta_{p,\,max}$) of 0.77 lm/W and the maximum external quantum efficiency ($\eta_{ext,\,max}$) of 1.53 %. In the contrast, the device A of BAB and BAC shows the maximum luminance efficiency of only 0.11 cd/A and 0.61 cd/A because of the deep HOMO result in the unmatched level with PEDOT:PSS and unbalanced of the hole and electron. The low turn-on voltage indicates an efficient and balanced charge injection, transport and recombination, most likely due to the HOMO energy levels of CAC being better matched with the PEDOT:PSS and the hole-transporting carbazole moiety increasing carrier balance in the emitting layer may also contribute to the high performance. The excellent performance is also probably due to the excellent thermal stability of the CAC, which significantly enhances the capability of forming stable amorphous thin films. The unsatisfactory performance of BAB based device A on account of the BAB bad solubility in CH_2Cl_2 among these molecules. Fig. 6 (c) reveals the identical electroluminescent spectra with deep-blue emission wavelength at 444, 448 and 448 nm of device A, respectively. The result also implies that CAC,

View Article Online
DOI: 10.1039/C5RA00627A

BAB and BAC should be a potential candidate for stable deep-blue fluorescent OLEDs materials.

To further improve the performance of the device, CAC, BAB and BAC were doped in PVK:OXD-7 (7:3) as emitting layer, respectively. We fabricated device B with an architecture of ITO/PEDOT:PSS(30 nm)/PVK:OXD-7(7:3):EML(5 wt%, 10 wt%, 15 wt%, 20 wt%)(20 nm)/TPBI(35 nm)/Ca(10 nm):Ag(100 nm). The devices' performances are presented in **Fig. 7** with the key parameters summarized in **Table 2**. Device B doped with BAB shows the highest turn-on voltage than CAC and BAC, which decreased with the increase of BAB doping concentration. The maximum electrochemical properties value of device B with 5 % doping concentration is similar to that of the device B with 10 % doping concentration, while device B with 15 % doping concentration shows higher efficiency over all current density range. For instance, the device B with 15 % doping concentration displays the $\eta_{c,\,max}$ of 0.67 cd/A and the $\eta_{ext,\,max}$ of 0.60 %, while the 5 %, 10 % and 20 % doping concentration devices show the $\eta_{c,\,max}$ of 0.55, 0.57 and 0.42 cd/A, and the $\eta_{ext,\,max}$ of 0.50, 0.52 and 0.38 %, respectively. Furthermore, device B doped CAC and BAC have the similar trends on the doping concentration change and the OLEDs performance. For example, the device B doped BAC with 15 % doping concentration shows the $\eta_{c,\,max}$, $\eta_{p,\,max}$ and $\eta_{ext,\,max}$ of 1.00 cd/A, 0.36 lm/W and 0.73 %, which displays the best performance during four various doping concentration. The devices of compounds with the hole-transporting carbazole moiety, CAC and BAC, show better performance than the BAB devices. Especially, the device B doped CAC has the best performance among

View Article Online
DOI: 10.1039/C5RA00627A

these diverse devices. For instance, the device B doped CAC with 15 % doping concentration shows the $\eta_{c,\,max}$, $\eta_{p,\,max}$ and $\eta_{ext,\,max}$ of 3.03 cd/A, 1.64 lm/W and 2.81 % better than all other devices. The device also has a low turn-on voltage of 4.75 V and a high L_{max} of 3490 cd/m^2. Device B of CAC shows the best electroluminescent characteristics can be attributed to the highest film fluorescence quantum efficiency (Φ_F) of CAC. This result is also consistent with the view that the introduction of the hole-transporting carbazole moiety into the fluorescent materials can balance charge injection, transport and recombination more efficiently which also contribute to the high performance. TPBI as electron transport layer can effective transmit electron so that the device contain BAB or BAC with electron-transporting benzimidazole moieties have weak capacity to balance the exciton recombination in the emitting layer. The electron-transporting material OXD-7 and the hole-transporting material PVK as host with appropriate mixing ratio in the emitting layer can enhance the exciton transport and recombination, which contribute to lowering the turn-on voltage, increasing the maximum brightness and improving the performance of deep-blue fluorescent OLEDs materials. As shown in table 2, the CIE coordinates are (0.16, 0.10), (0.17, 0.11) and (0.16, 0.11) for CAC, BAB and BAC, respectively, which were measured in device B with 15 % doping concentration. Fig. 7 (c) reveals the identical electroluminescent spectra with deep-blue emission wavelength at 448, 436 and 440 nm of device B, respectively. Furthermore, no additional emission coming from host materials was observed, indicative of efficient energy transfer from the host to the emitters.

View Article Online
DOI: 10.1039/C5RA00627A

Conclusion

In summary, we have designed and synthesized three novel materials CAC, BAB and BAC for solution-processed deep-blue fluorescent OLEDs. A series of devices based on these derivatives exhibit their excellent thermal and electrochemical stability, charge transport character, solubility and film-forming property. The calculated geometries of CAC and BAC show that the carbazole units are significantly twisted against the anthracene core, effectively suppressing molecular recrystallization and limit the extent of conjugation, which improves the morphological stability of the thin film. The hole-transporting carbazole moiety increasing carrier balance in the emitting layer may also contribute to the high performance. Herein, we fabricated solution-processed deep-blue fluorescence OLEDs with CAC as a dopant, and the device showed low turn-on voltage of 4.75 V, high efficiency of 3.03 cd/A, 1.64 lm/W, and a maximum external quantum efficiency of 2.81 %. According to these characteristics, these materials, especially CAC, have sufficient potential for use in deep-blue fluorescence OLED applications.

Acknowledgments

The authors thank the National basic Research Program China (2013CB932902) and National Natural Science Foundation of China (51103023, 21173042) for their financial support.

View Article Online
DOI: 10.1039/C5RA00627A

References

1 C. W. Tang and S. A. Vanslyke, *Appl. Phys. Lett.*, 1987, **51**, 913.
2 S. R. Forrest, *Nature*, 2004, **428**, 911.
3 B. W. D'Andrade and S. R. Forrest, *Adv. Mater.*, 2004, **16**, 1585.
4 C. C. Wu, Y. T. Lin, K. T. Wong, R. T. Chen and Y. Y. Chien, *Adv. Mater.*, 2004, **16**, 61.
5 A. J. Heeger, *Angew. Chem., Int. Ed.*, 2001, **40**, 2591.
6 Z. Q. Jiang, Z. Y. Liu, C. L. Yang, C. Zhong, J. G. Qin, G. Yu and Y. Q. Liu, *Adv. Funct. Mater.,* 2009, **19**, 3987.
7 M. R. Zhu and C. L. Yang, *Chem. Soc. Rev.*, 2013, **42**, 4963.
8 C. Fan, Y. Li, C. Yang, H. Wu, J. Qin and Y. Cao, *Chem. Mater.*, 2012, **24**, 4581.
9 H. Uoyama, K. Goushi, K. Shizu, H. Nomura and C. Adachi, *Nature*, 2012, **492**, 234.
10 K. Danel, T. H. Huang, J. T. Lin, Y.T. Tao and C.H. Chuen, *Chem. Mater.*, 2002, **14**, 3860.
11 C. H. Wu, C. H. Chien, F. M. Hsu, P. I. Shih and C. F Shu., *J. Mater. Chem.*, 2009, **19**, 1464.
12 C. H. Chien, C. K. Chen, F. M. Hsu, C. F. Shu, P. T. Chou and C. H. Lai, *Adv. Funct. Mater.*, 2009, **19**, 560.
13 J. Huang, J. H. Su, X. Li, M. K. Lam, K. M. Fuang, H. H. Fan, K. W. Cheah, C. H. Chen and H. Tian, *J. Mater. Chem.*, 2011, **21**, 2957.
14 M. H. Tsai, H. W. Lin, H. C. Su, T. H. Ke, C. C. Wu, F. C. Fang, Y. L. Liao, K. T. Wong and C. I. Wu, *Adv. Mater.*, 2006, **18**, 1216.
15 S. O. Jeon, K. S. Yook, C. W. Joo and J. Y. Lee, *Adv. Mater*., 2011, **22**, 1872.
16 W. Jiang, L. Duan, J. Qiao, L. D. Wang and Y. Qiu, *Org. Lett.*, 2011, **13**, 3146.
17 Y. Tao, Q. Wang, C. Yang, Q. Wang, Z. Zhang, T. Zou, J. Qin and D. Ma, *Angew. Chem., Int. Ed.,* 2008, **47**, 8104.
18 W. J. Kuo, S. L. Lin, S. D. Chen, C. P. Chang, R. H. Lee and R. J. Jeng, *Thin Solid Films*, 2008, **516**, 4145.
19 I. Cho, S. H. Kim, J. H. Kim, S. Park and S. Y. Park, *J. Mater. Chem.*, 2012, **22**, 123.
20 P. Kundu, K. R. J. Thomas, J. T. Lin, Y. T. Tao and C. H. Chien, *Adv. Funct. Mater.*, 2003, **13**, 445.
21 K. R. J. Thomas, J. T. Lin, Y. T. Tao and C. W. Ko, *J. Am. Chem. Soc.*, 2001, **123**, 9404.
22 G. Hughes and M. R. Bryce, *J. Mater. Chem.*, 2005, **15**, 94.
23 J. H. Kim, D. Y. Yoon, J. W. Kim and J. J. Kim, *Synth. Met.,* 2007, **157**, 743.
24 Y. Shirota and H. Kageyama, *Chem. Rev.*, 2007, **107**, 953.
25 C. H. Chen, W. S. Huang, M. Y. Lai, W. C. Tsao, J. T. Lin, Y. H. Wu, T. H. Ke, L. Y. Chen and C. C. Wu, *Adv. Func. Mater.*, 2009, **19**, 2661.
26 *Gaussian 03 (Revision B.05)*, Gaussian, Inc., Wallingford CT, 2004.
27 W. Jiang, J. N. Tang, X. X. Ban, Y. M. Sun, L. Duan and Y. Qiu, *Org. Lett.*, 2014, **16**, 5346.

View Article Online
DOI: 10.1039/C5RA00627A

28 H. Zhang, S. Wang, Y. Li, B. Zhang, C. Du, X. Wan and Y. Chen, *Tetrahedron*, 2009, **6**, 4455.
29 K. Albrecht and K. Yamamoto, *J. Am. Chem. Soc.*, 2009, **131**, 2244.
30 M. Smet, J. V. Dijk and W. Dehaen, *Tetrahedron*, 1999, **55**, 7859.
31 I. B. Berlan, Handbook of fluorescence spectra of aromatic molecules. 2nd ed. New York: Academic, 1971.

View Article Online
DOI: 10.1039/C5RA00627A

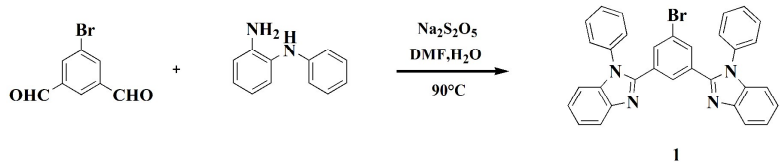

1

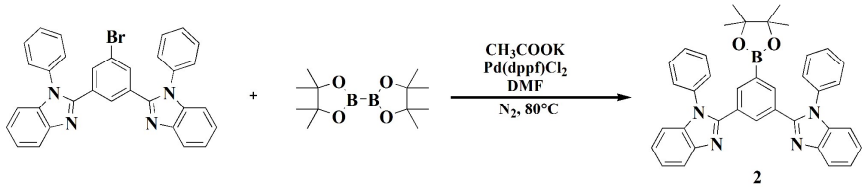

2

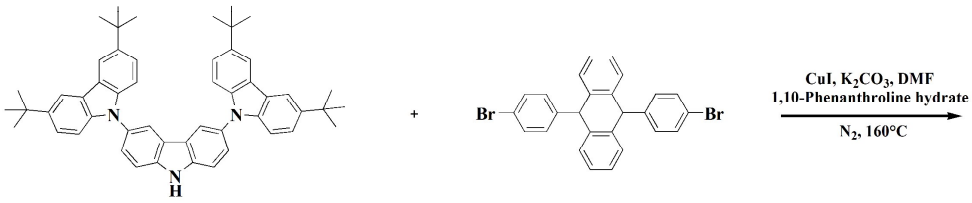

3 4

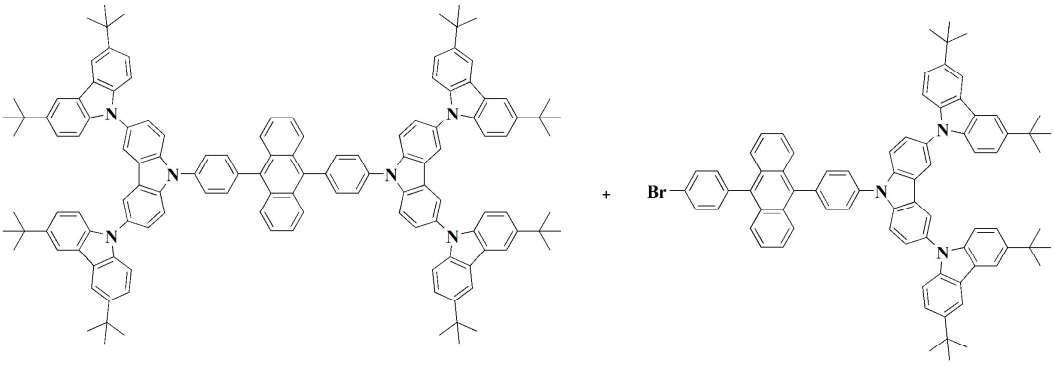

CAC 5

View Article Online
DOI: 10.1039/C5RA00627A

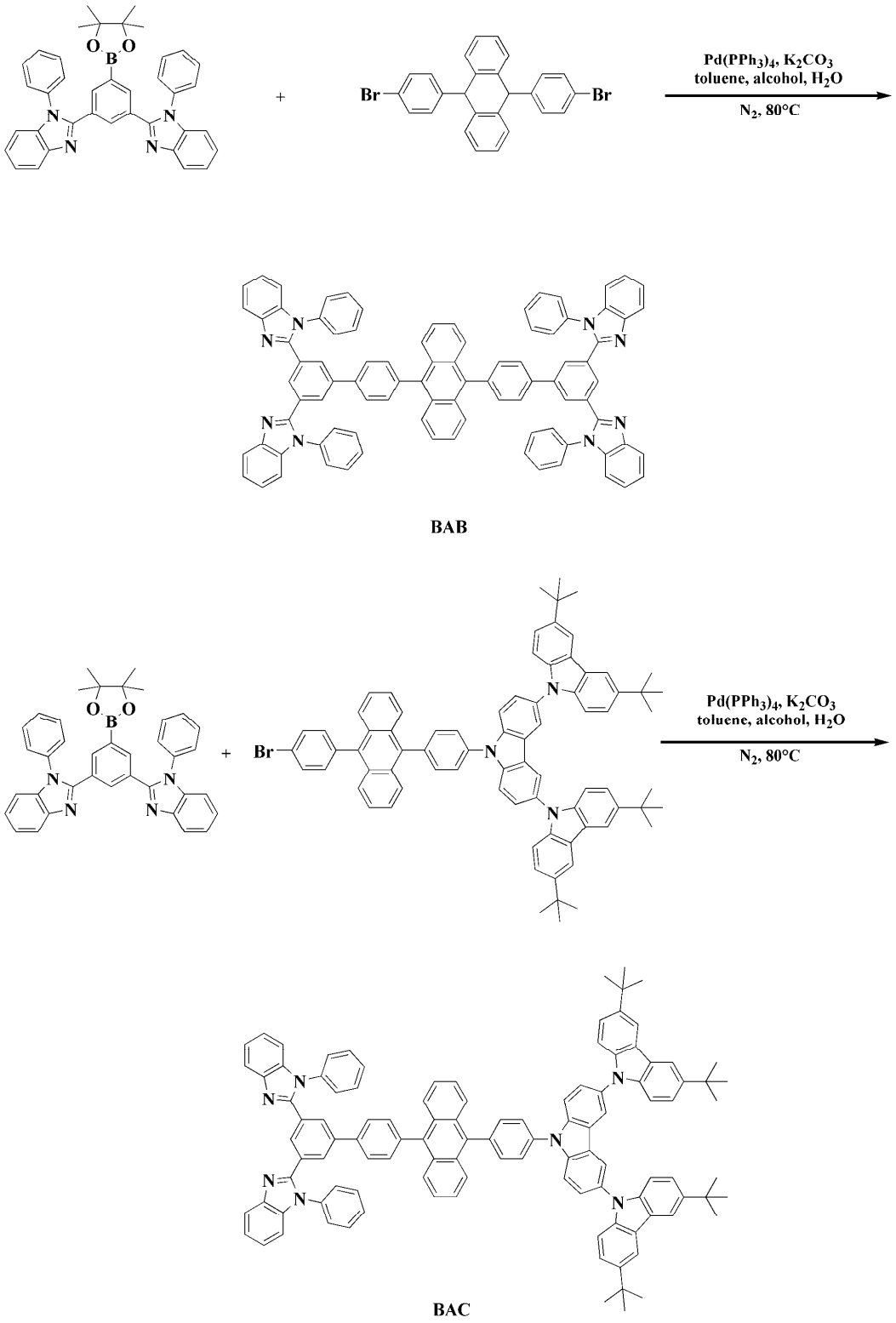

Scheme 1 Synthetic routes toward CAC, BAB, and BAC.

Compd.	T_g/T_d[a] (°C)	λ_{abs}[b] (nm)	λ_{em}[b] (nm)	λ_{em}[c] (nm)	Φ_F[c]	E_g[d] (eV)	E_g Calcd [e] (eV)	HOMO/ LUMO[e] (eV)	HOMO/ LUMO[f] (eV)
CAC	-/508	242/298/351/376/396	435	439	0.87	3.00	3.01	-5.04/-2.03	-5.23/-2.25
BAB	195/534	263/298/358/377/397	430	439	0.59	2.97	3.47	-5.11/-1.64	-5.87/-2.88
BAC	246/494	242/262/298/356/377/397	434	442	0.70	2.98	3.15	-5.00/-1.85	-5.26/-2.26

[a] Measured by DSC/TGA at a heating rate of 10 °C min^{-1}.[b] Measured in CH_2Cl_2.[c] Measured in thin film on quartz substrate. [d] Estimated from the optical absorption edge, $E_g = 1240/\lambda_{onset}$.[e] Obtained from quantum calculations by using B3LYP/6-31G(d).[f] Calculated by HOMO = –(4.8 + E^{OX}_{onset}), and LUMO = HOMO+ E_g, where E^{OX}_{onset} is the onset potential of the oxidation.

Table 1 Physical data of the materials.

Device	emitter	V_{on}[a] (V)	L_{max}[b] (cd/m^2)	$\eta_{c,max}$[c] (cd/A)	$\eta_{p,max}$[d] (lm/w)	$\eta_{ext,ma}$[e] (%)	Devices@100cd/m^2			Devices@1000cd/m^2			CIE (x, y)[f]
							η_c (cd/A)	η_p (lm/w)	η_{ext} (%)	η_c (cd/A)	η_p (lm/w)	η_{ext} (%)	
A	CAC	4.91	3983	1.63	0.77	1.53	1.35	0.69	1.26	1.46	0.61	1.37	(0.16, 0.10)
	BAB	5.80	400	0.11	0.04	0.10	0.10	0.04	0.09	-	-	-	(0.22, 0.22)
	BAC	5.49	2945	0.61	0.27	0.47	0.60	0.27	0.46	0.40	0.13	0.31	(0.18, 0.16)
B[g]	CAC 5%	4.92	2826	1.53	0.60	1.41	1.23	0.55	1.14	1.27	0.39	1.17	(0.16, 0.10)
	CAC 10%	4.89	3476	1.95	0.89	1.80	1.94	0.85	1.79	1.68	0.54	1.56	(0.17, 0.12)
	CAC 15%	4.75	3490	3.03	1.64	2.81	3.01	1.39	2.78	2.22	0.71	2.05	(0.16, 0.10)
	CAC 20%	4.30	2970	1.96	1.03	1.81	1.95	0.90	1.80	1.48	0.49	1.37	(0.16, 0.10)
	BAB 5%	7.64	874	0.55	0.20	0.50	0.48	0.14	0.43	-	-	-	(0.16, 0.09)
	BAB 10%	7.36	1212	0.57	0.22	0.52	0.67	0.21	0.60	0.44	0.11	0.40	(0.18, 0.13)
	BAB 15%	6.42	1425	0.67	0.23	0.60	0.57	0.20	0.52	0.44	0.12	0.40	(0.17, 0.11)
	BAB 20%	7.01	998	0.42	0.14	0.38	0.39	0.14	0.35	-	-	-	(0.17, 0.11)
	BAC 5%	6.40	1608	0.68	0.20	0.50	0.43	0.15	0.31	0.61	0.15	0.44	(0.16, 0.10)
	BAC 10%	6.68	1359	0.75	0.28	0.55	0.75	0.26	0.54	0.44	0.11	0.32	(0.17, 0.11)
	BAC 15%	6.97	1711	1.00	0.36	0.73	1.00	0.33	0.72	0.66	0.16	0.48	(0.16, 0.11)
	BAC 20%	6.99	1983	0.74	0.26	0.53	0.73	0.26	0.53	0.57	0.15	0.41	(0.16, 0.11)

[a]Recorded at 1 cd/m^2.[b]Maximum luminance at applied voltage.[c]Maximum current efficiency.[d] Maximum power efficiency. [e]Maximum external quantum efficiency.[f]Data were measured at 10 V.[g]CAC, BAB and BAC doped in PVK:OXD-7, respectively.

Table 2 Electroluminescent performance.

View Article Online
DOI: 10.1039/C5RA00627A

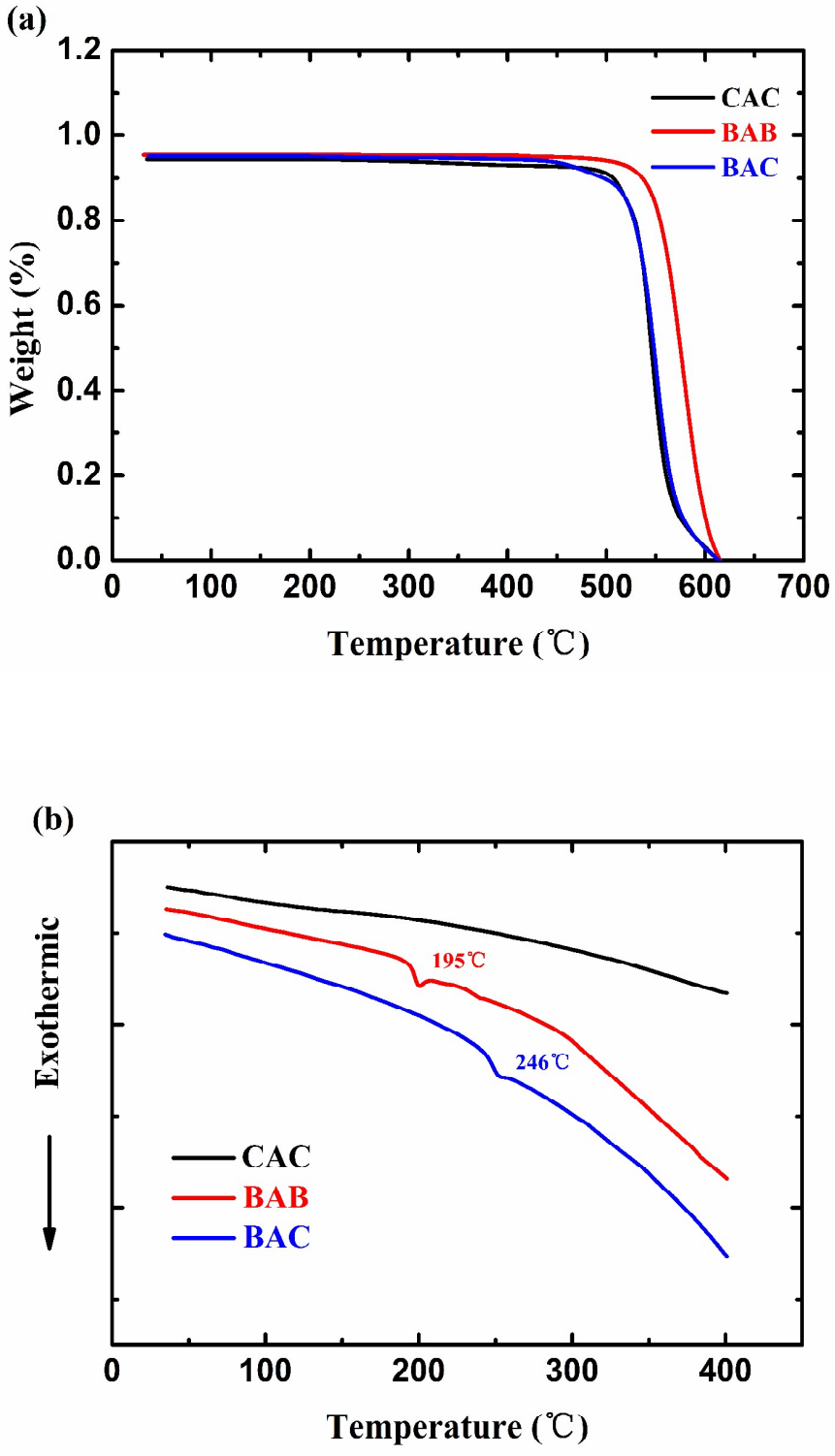

Fig. 1 (a) TGA traces of CAC, BAB and BAC recorded at a heating rate of 10 °C min^{-1}. (b) DSC measurement recorded at a heating rate of 10 °C min^{-1}.

View Article Online
DOI: 10.1039/C5RA00627A

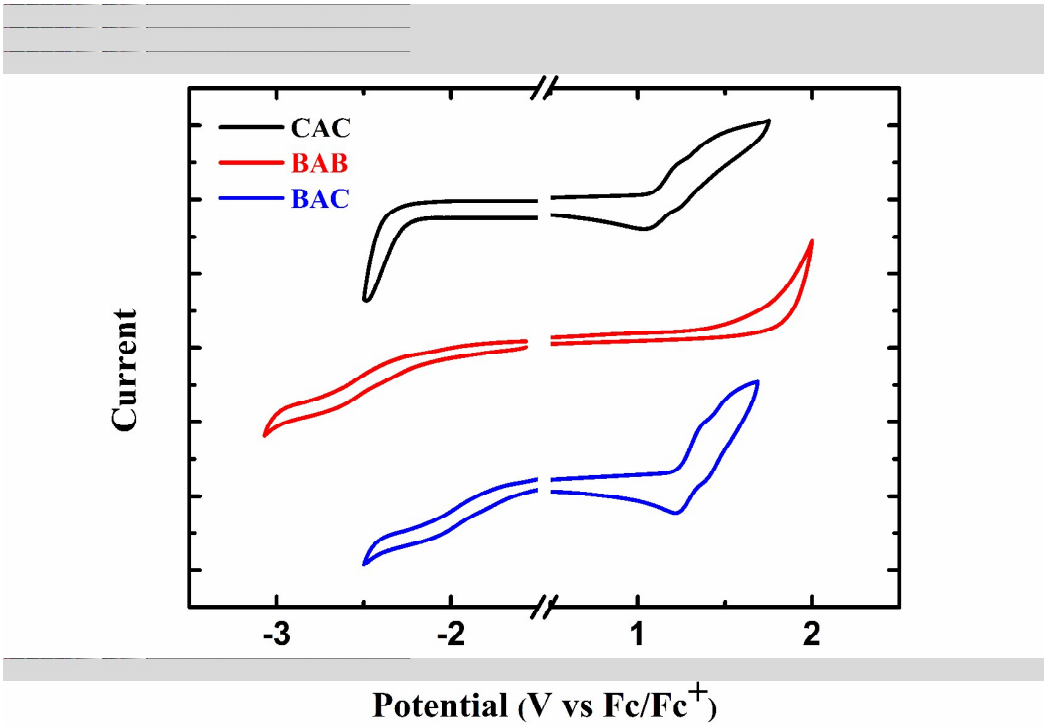

Fig. 2 Electrochemical properties of CAC, BAB and BAC.

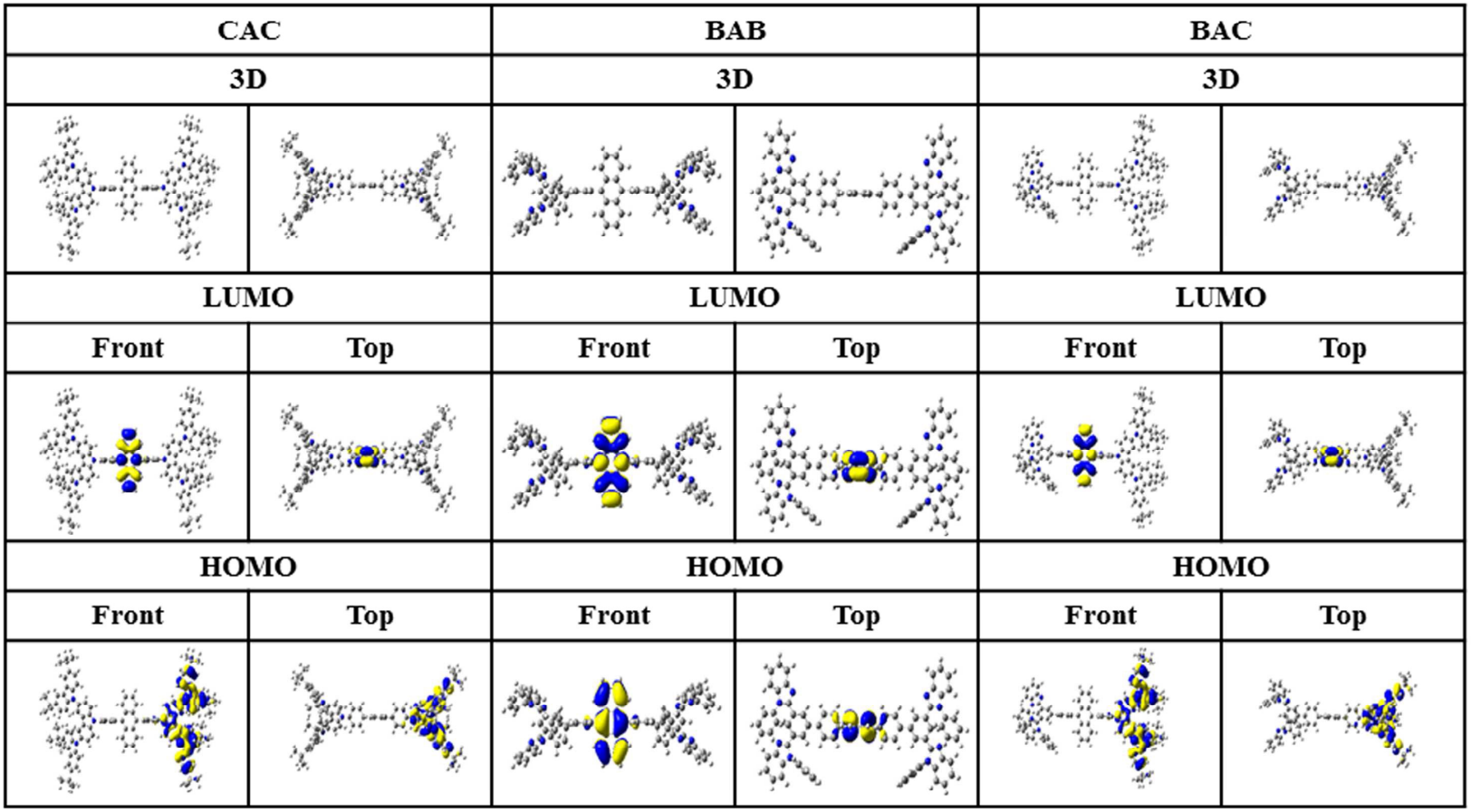

Fig. 3 Optimized geometries and calculated HOMO and LUMO density maps for CAC, BAB and BAC according to DFT calculations at the B3LYP/6-31* level.

View Article Online
DOI: 10.1039/C5RA00627A

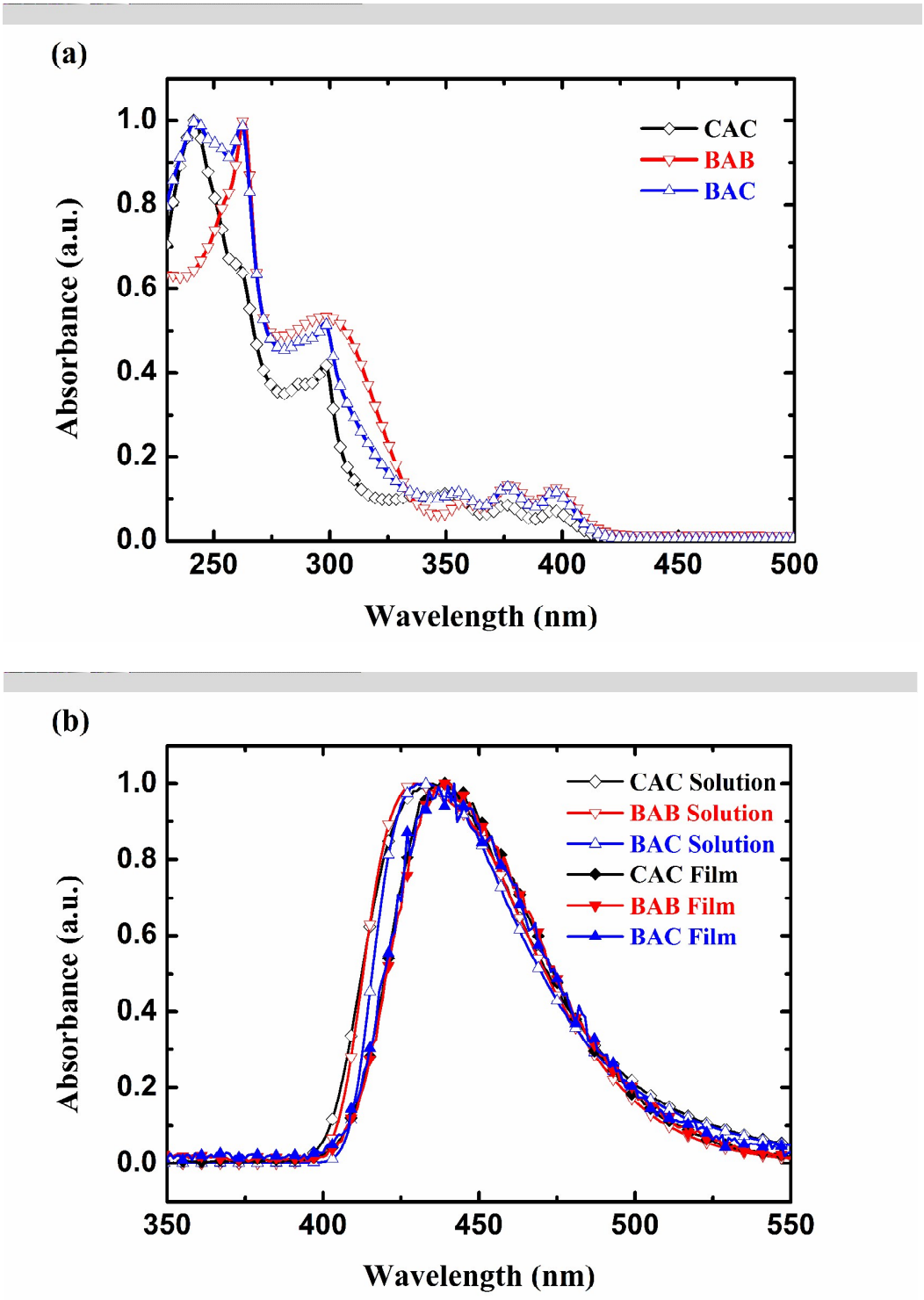

Fig. 4 Normalized absorption (a) and emission (b) spectra of CAC, BAB and BAC in dilute dichloromethane solution and solid film.

View Article Online
DOI: 10.1039/C5RA00627A

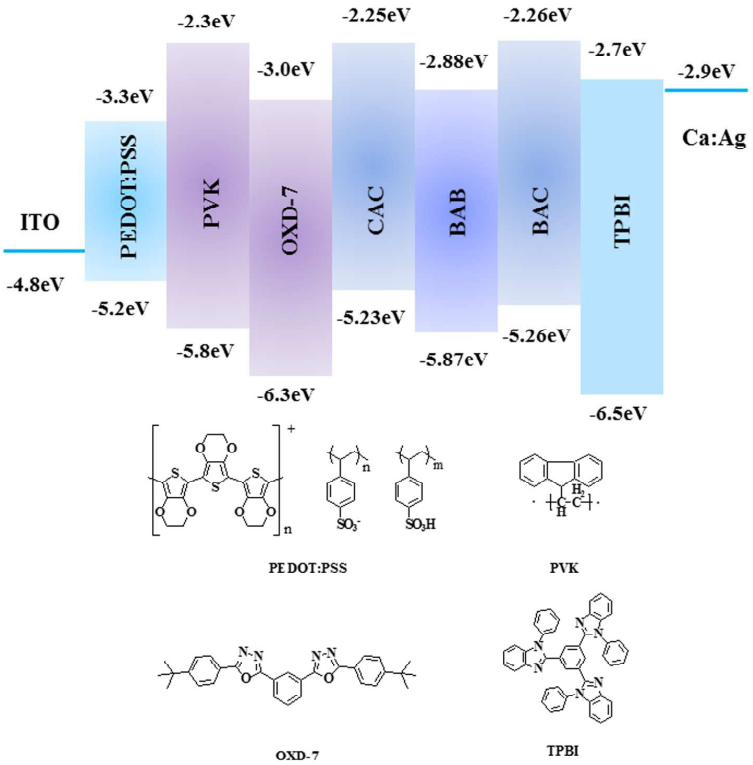

Fig. 5 Structure of the materials in the devices and energy-level diagrams.

View Article Online
DOI: 10.1039/C5RA00627A

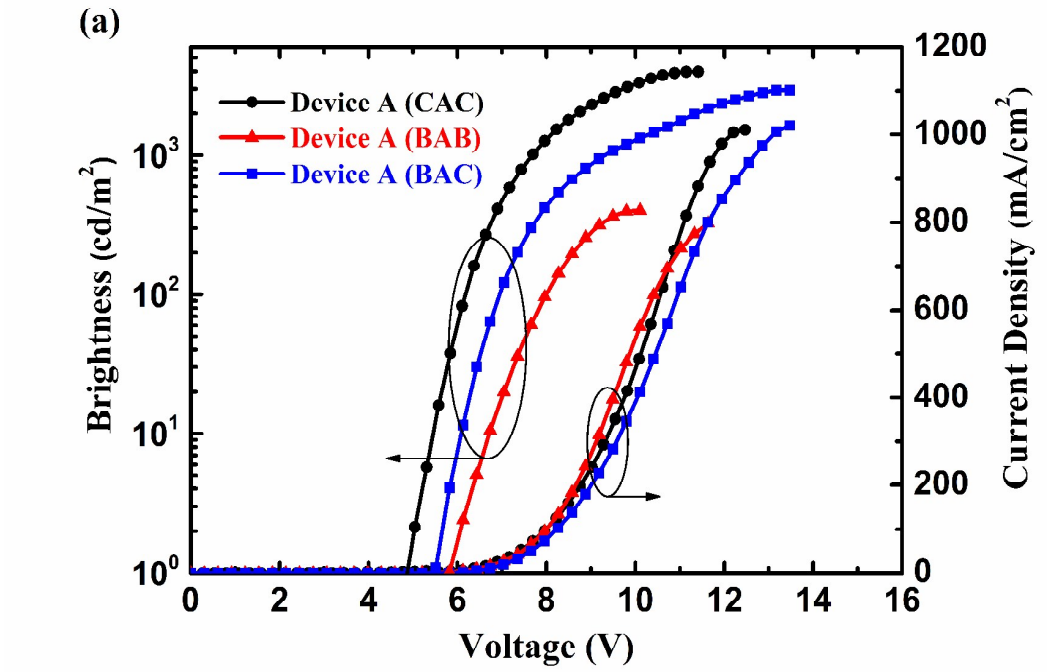

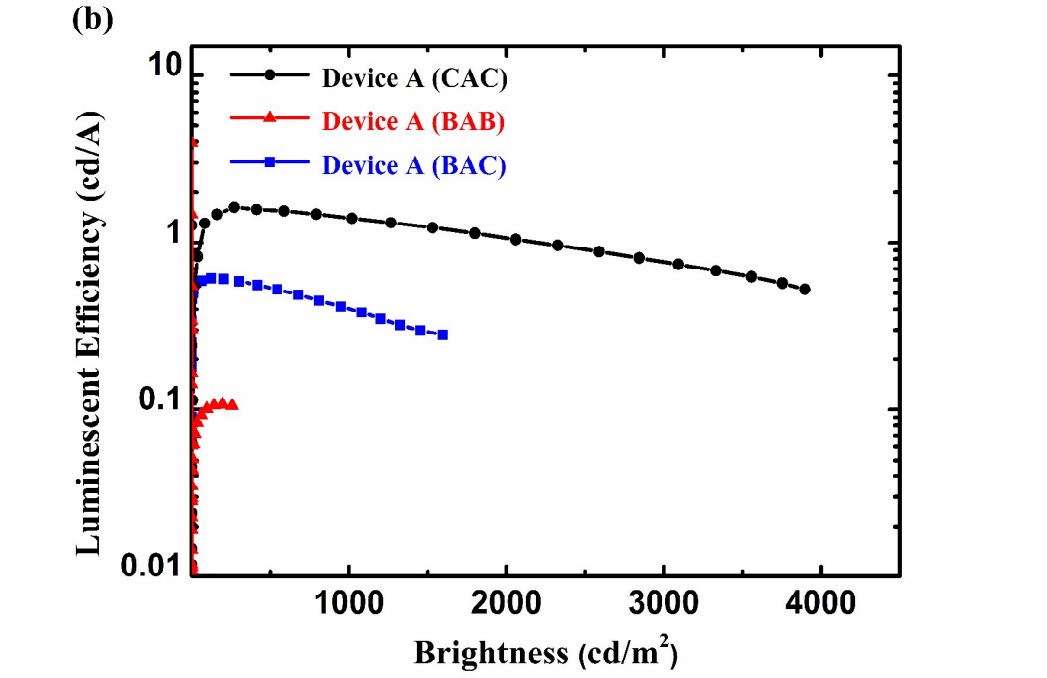

View Article Online
DOI: 10.1039/C5RA00627A

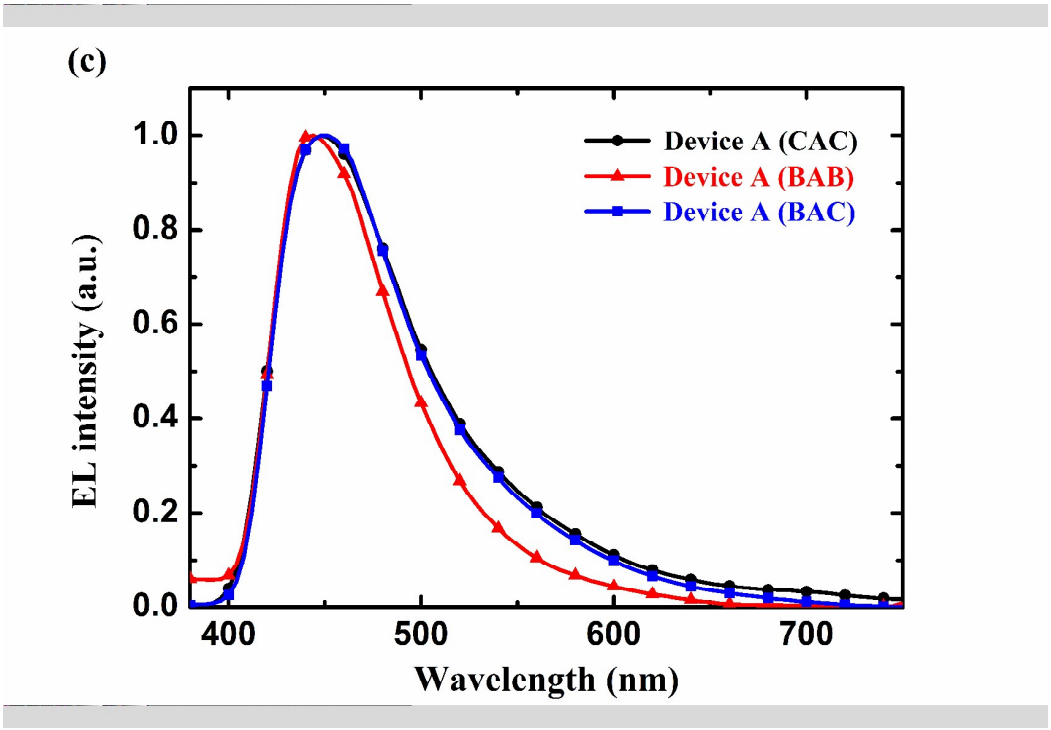

Fig. 6 The EL performance of CAC, BAB and BAC based device A, (a) current density-voltage-luminance (J-V-L) (b) brightness-luminescent efficiencies curves (c) the normalized EL spectra of devices at a driving voltage of 10 V.

View Article Online
DOI: 10.1039/C5RA00627A

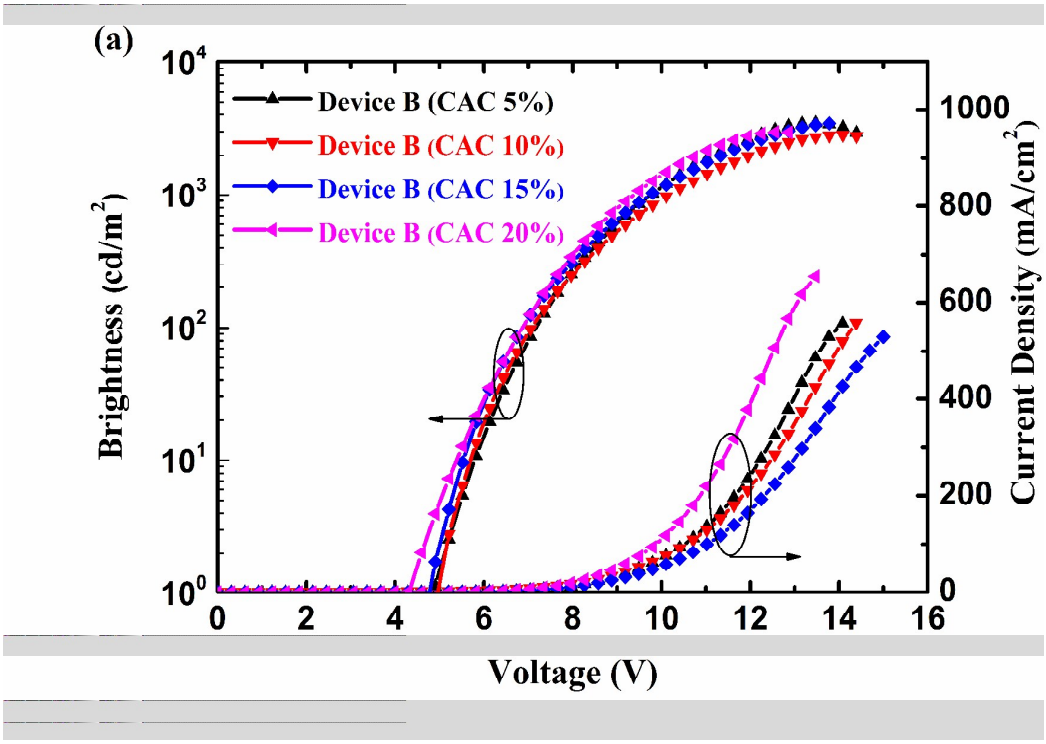

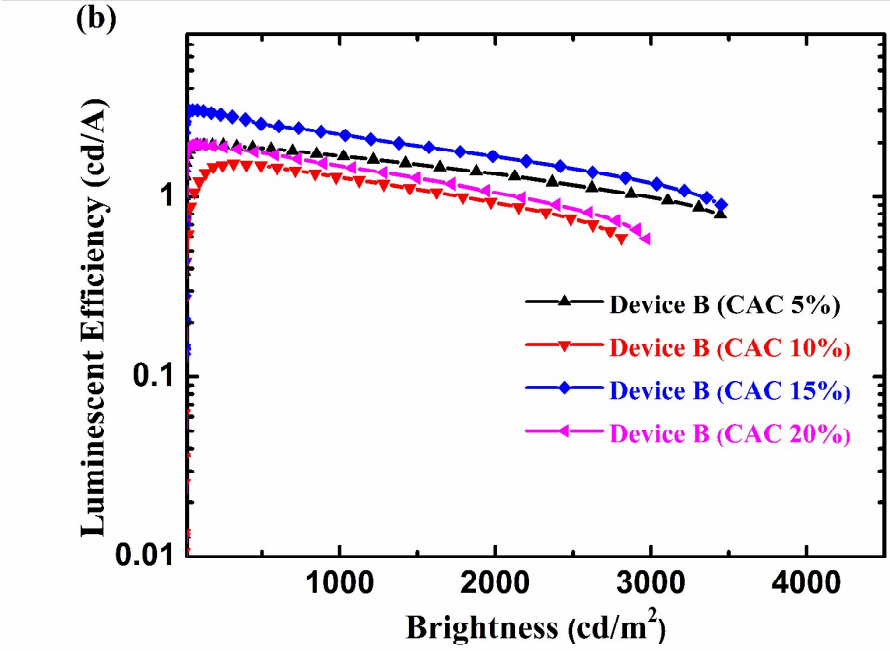

View Article Online
DOI: 10.1039/C5RA00627A

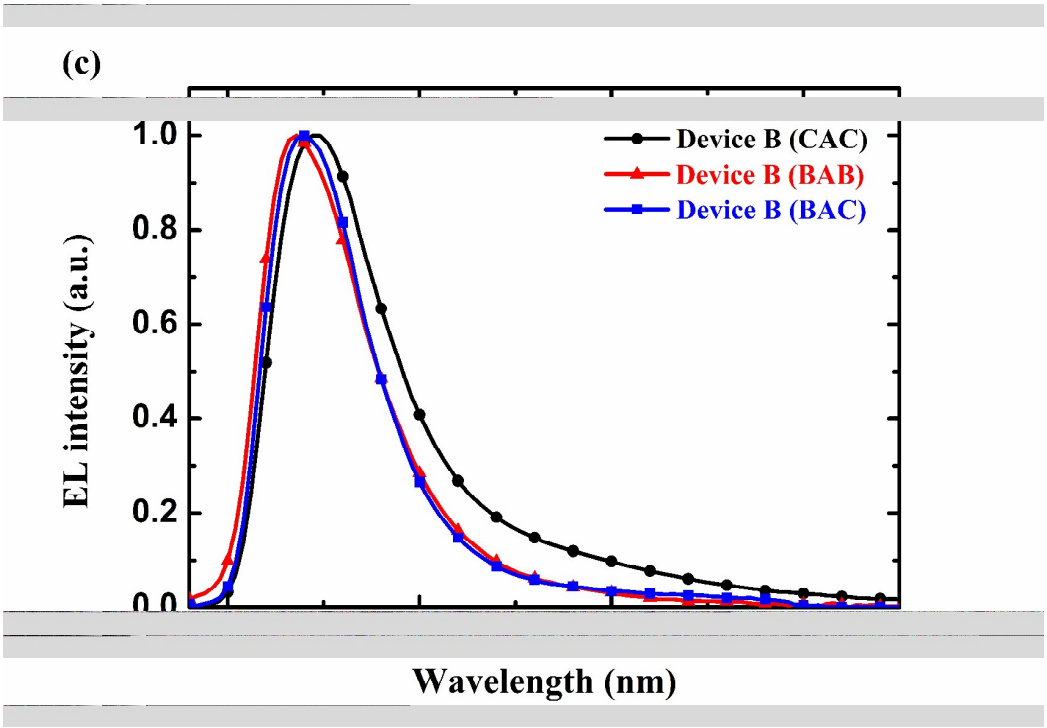

Fig. 7 The EL performance of CAC based device B, (a) current density-voltage-luminance (J-V-L) (b) brightness-luminescent efficiencies curves (c) the normalized EL spectra of CAC, BAB and BAC based device B with 15% doping concentration at a driving voltage of 10.

View Article Online
DOI: 10.1039/C5RA00627A

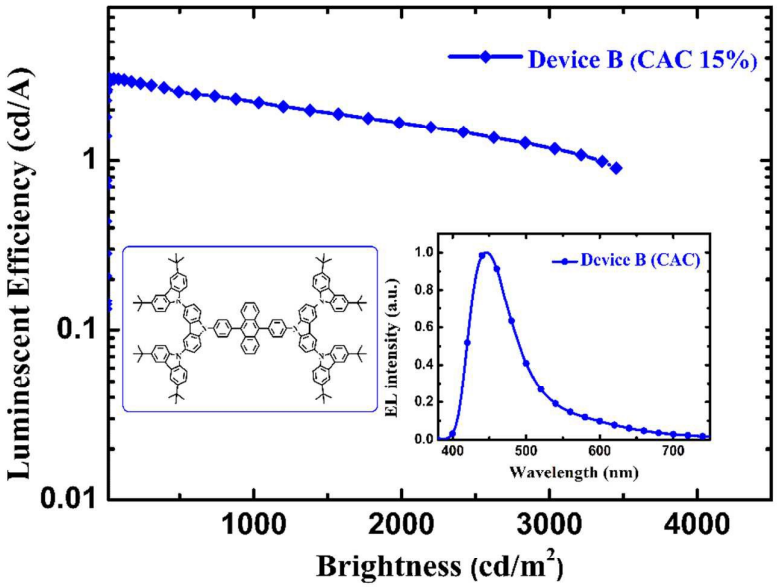

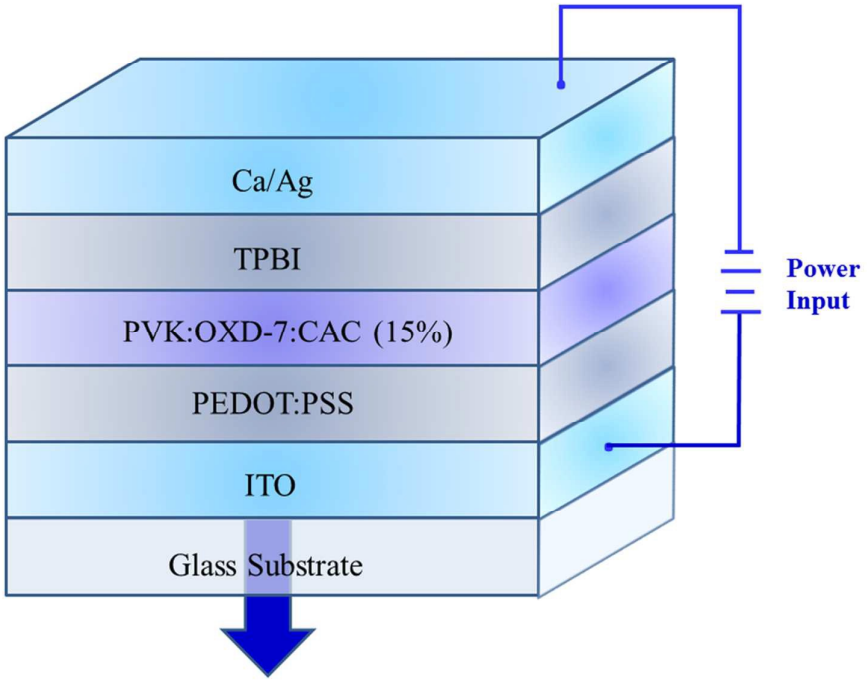

Graphic Abstract

Carbazole substituted 9,10-diphenyl-anthracene derivatives used in deep-blue fluorescence OLED materials with excellent performance.